Alternative Approach for Efficiency Data Generation in Neutron Activation Analysis

R.L. Njinga
Physics Department
Ibrahim Badamasi Babangida University
Lapai, Niger State, Nigeria

I.O.B. Ewa
Center for Energy Research and Training
Ahmadu Bello University
Zaria, Nigeria

S.A., Jonah
Center for Energy Research and Training
Ahmadu Bello University
Zaria, Nigeria

A. Baba
Physics Department
Ibrahim Badamasi Babangida University
Lapai, Niger State, Nigeria

Y.A. Ahmed
Center for Energy Research and Training
Ahmadu Bello University
Zaria, Nigeria

G.A. Agbo
Center for Energy Research and Training
Ahmadu Bello University
Zaria, Nigeria

J. Ebobenow
Physics Department
University of Buea, South West Region
Republic of Cameroon

R. Nasiru
Physics Department
Ahmadu Bello University,Zaria
Kaduna State, Nigeria

Abstract

An efficiency calibration method has been developed to measure radioactivity of samples instantly with HPGe detectors without the continuous usage of standards sources. A co-axial HPGe detector was used for this experiment and the geometries of 17cm, 15cm and 2cm examined. Three fundamental techniques viz k_0-IAEA, theoretical (fitted) and experimental measurements were used to examine and actualize this method known as effective solid angle derived efficiency technique within the energy range of 59.54 – 1408 keV. Plotted ratios of the k_0-IAEA derived efficiency, theoretical (fitted) derived efficiency, and experimental full energy peak derived efficiency values over the instant effective solid angle derived efficiency values showed slight oscillations about unity at certain energies for 2cm and 17cm geometries attributed to the characteristics of the detector. The results of the ratio of k_0-IAEA measurement, theoretical (fitted) derived efficiency data over the experimentally derived efficiency at 15cm showed an insignificant deviation of 0.2% at certain energy around the unity mark. Thus efficiency data obtained at this geometry were employed in the instant effective solid angle efficiency transfer technique and further determination of the instant efficiency at 1, 5, 10, 15, 20, and 25cm were obtained.

Keywords: k_0-IAEA, full energy peak efficiency, HPGe detector, standard sources

1. Introduction

The need for a fast, instant analytical method for Instrumental Neutron Activation Analysis (INAA) is obvious in view of the wide application of the technique in multi-elemental analysis. The availability of Standard Reference Material in efficiency calibration from agencies like the National Institute of Standards and Technology (NIST), the United State Geological Services (USGS), and the International Atomic Energy Agency (IAEA) and other national bodies make the distribution fairly late or fairly easy for users. This work seeks to address a novel method that does not rely solely on the use of standard point sources at all times.

Since the Miniature Neutron Source Reactor (MNSR) in Center for Energy Research and Training (CERT), Ahmadu Bello University (ABU) Zaria-Nigeria achieved criticality on February 3, 2004 and commissioned for training and research Jonah et al., (2005) the spectrum of work to be analyzed on daily routine is increasing spontaneously. The fundamental analytical approach in obtaining elemental concentrations basically used in the Neutron Activation Analysis laboratory are k_o-Neutron Activation Analysis (k_o-NAA) and k_o-EpiCd Neutron Activation Analysis techniques (k_o-ENAA) as shown in eq. (1) and (2) respectively. Both techniques (eq. 1 & 2) confirmed firmly the reliability on the efficiency calibration values at specific counting positions called geometries as illustrated below (De Corte et al., 2004) ;

$$conc\left(a\right) = \frac{\left(\dfrac{N_p}{t_m SDCW}\right)_a}{\left(\dfrac{N_p}{t_m SDCW}\right)_m} \times \frac{1}{k_{o,m}\left(a\right)} \times \frac{f + Q_{O,m}\left(\alpha\right)}{f + Q_{O,a}\left(\alpha\right)} \times \frac{\varepsilon_{\gamma,m}}{\varepsilon_{\gamma,a}} \qquad (1)$$

$$conc\left(a\right) = \frac{\left(\dfrac{(N_p)_{Cd}}{t_m SDCW}\right)_a}{\left(\dfrac{(N_p)_{Cd}}{t_m SDCW}\right)_m} \times \frac{1}{k_{o,m}\left(a\right)} \times \frac{F_{Cd,m} Q_{O,m}\left(\alpha\right)}{F_{Cd,a} Q_{O,a}\left(\alpha\right)} \times \frac{\varepsilon_{\gamma,m}}{\varepsilon_{\gamma,a}} \qquad (2)$$

where the subscripts "a" and "m" stands respectively for the analyte and the co-irradiated monitors, ε_γ is the efficiency calibration values, N_p the net peak count corrected for pulse losses, t_m the measuring time, $k_{o,m}\left(a\right)$ the k_0 factors of "a" and "m", and F_{Cd} the cadmium transmission factor for epithermal neutrons. For radioactivity measurement, the gamma-ray spectrometry with a High Purity Germanium (HPGe) coaxial detector is widely used (Owens, 1989). A detection efficiency curve, that is, a set of photopeak efficiencies over the energy region of interest must be known in advance for the geometries of measurements. Notwithstanding, energy calibration is required to be carried on once a week or in two weeks. So spectrometry users have to pay much money for these sources. An efficiency calibration method has been developed in this work to measure radioactivity of samples instantly with HPGe detectors without the continuous usage of standards sources. In order to obtain the authenticity and assurance of the technique, three fundamental techniques viz k_0-IAEA efficiency evaluation technique, theoretical or fitted efficiency technique and experimental efficiency measurements technique were used to examine and actualize this method known as effective solid angle derived efficiency technique within the stipulated energy range of 59.54 – 1408 keV.

In the experimental measurements technique, different geometries were employed with active calibrating matrix i.e. standard point sources of photon energy line. The energy line (gamma ray) employed in this work were limited to gamma energy having emission probability greater than 13% and is as shown in the Table 1 below.
In the case of the k_0-IAEA, the International Atomic Energy Agency (IAEA) via technical cooperation and Coordinated Research Projects (CRP), expert services, and fellowship awards developed this nondestructive, multi-element determination method with a high degree of accuracy and reliability. This method is well established in the nuclear analytical community all over the world. In like manner, the k_0-IAEA was used in this work to evaluate the full energy peak efficiency of the high purity germanium detector using the single point source [152]Eu with several gamma emission lines. The results will be compared with the solid angle efficiency transfer technique.

Insert table (1) about here

2. Experimental

2.1 Experimental Efficiency Measurements Technique

The coaxial HPGe detector (ORTEC ©) Model number "GEM-30195" with performance specifications used for the investigation are listed in Table 2 below.

Insert table (2) about here

The five radionuclide sources ^{241}Am, ^{226}Ra, ^{60}Co, ^{137}Cs, and ^{152}Eu used were counted for 3600 second at each instant. After accumulating sufficient counts by an MCA for each of the peaks with respect to the sources, the MAESTRO emulation software program was used to obtained the net full peak (background subtracted) counts for each photon of interest with gamma ray emission probability of 13% and above. The activity of each sources were normalized to the measurement date before obtaining the full energy peak efficiency ε for a particular sample-to-detector geometry. The full energy peak efficiency was performed practically by employing the formula given as (ANSI/IEEE, 1996);

$$\varepsilon = \frac{A_D}{ER C_{SA} C_{SE}} \tag{3}$$

where C_{SA} and C_{SE} are the respective correction factors for self-absorption and summing effect, A_D the count rate, and ER the emission rate. The full energy peak efficiencies of the detector for all the distances were evaluated and the results are shown in Table 4-6.

2.2   Effective Solid Angle Derived Efficiency Technique

Gamma rays (photons) are generally emitted equally in all directions thereby covering a solid angle for a point source positioned at geometry "d" defined as (Debertin and Helmer, 1988);

$$\text{Solid angle } \Omega(d) = 2\pi \left[1 - \left(1 + \frac{R_D^2}{d^2} \right)^{-\frac{1}{2}} \right] \tag{4}$$

where $\Omega(d)$ is the effective solid angle, d the specific geometry, and R_D the radius of the detector end cap.

The buildup of full energy peak efficiency ε is governed by the proportion of the intercepted space by the detector active area (A) given as expressed in eq. (5). Investigation was made in relation to the solid angle generated and the detector active area within 1-25cm distances from the detector end-cap and the result is shown in Table 8. The variation of solid angle generated and the distances has been discussed elsewhere (Njinga, *et al.,* 2009).

$$\text{Detector active area (A)} = 2\pi d^2 \left[1 - \left(\frac{d^2}{d^2 + R_D^2} \right)^{\frac{1}{2}} \right] \tag{5}$$

The experimental efficiency curve was basically used as the reference efficiency curve for the solid angle method since it yielded good results with little uncertainties and is widely accepted. Thus, the FEPE values obtained experimentally at a particular distance $\varepsilon(d_i)$ was used to validate efficiency $\varepsilon(d_j)$ at another position d_j instantly by means of experimentally derived efficiency. This was obtained from the concept of the solid angle buildup $\Omega(d_i)$ and $\Omega(d_j)$ for the two positions expressed as;

$$\varepsilon(d_j) = \left(\left[\frac{A_D}{ER C_{SA} C_{SE}} \right]_{d_i} \right) \times \left(\left[1 - \left(1 + \frac{R_D^2}{d^2} \right)^{-\frac{1}{2}} \right]_{d_j} \right) \times \left[1 - \left(1 + \frac{R_D^2}{d^2} \right)^{-\frac{1}{2}} \right]_{d_i}^{-1} \tag{6}$$

All symbols retain initial meanings; where $i = 1,2,3,...$ and $j = 1,2,3,...$

2.3   Theoretical (fitted) Efficiency Evaluation Technique

Full Energy Peak Efficiency (FEPE) may also be expressed theoretically in form of a polynomial with respect to gamma energy E as (Ewa et al., 2002):

$$\log(\varepsilon) = \sum_{j=0}^{n} a_j \left(\log E / E_0\right)^j \tag{7}$$

where ε is the FEPE, a_j are constants and E_0 set at 1keV, thereby making the quantity E, photon energy in keV. The coefficients a_j may be obtained for each distance by fitting Eq. (7) to the experimental efficiency values for that particular distance[10]. In other to obtain the coefficients $a_j(d)$ for each of the distances, the experimentally measured efficiency data for the different geometries were fitted with the theoretical function Eq. (7). Since not all the full energy range of 59.5-1408 KeV can be covered with a single polynomial, the range was divided into two portions $50 \leq E \leq 200\,\text{KeV}$ and $200 < E \leq 1408\,\text{KeV}$ respectively. Within the $50 \leq E \leq 200\,\text{KeV}$ portion, the second order polynomial in energy, E was used and fitted the measured efficiency data (Kamboj and Kahn, 1994);

$$\varepsilon = \sum_{j=0}^{2} a_j(d) E^j \tag{8}$$

While for the $200 < E \leq 1408$ KeV region, a power function of 1st order polynomial in log E were used to fit the measured efficiency data (Debertin et al, 1976)

$$\log \varepsilon = \log \left[a_0(d)\right] + a_1(d) \log \left(\frac{E}{E_0}\right) \tag{9}$$

The values obtained from the fit for the different positions 17cm, 15cm, and 2cm are shown in Table 3. The solid line curves obtained from the data generated which are superimposed with the curves derived from techniques are shown in Fig. 1-3.

2.4 k_0-IAEA Efficiency Calibration Technique

The detector's dimensions; crystal diameter 58.8mm, crystal length 76.3mm, end cap to crystal 3mm, aluminum absorbing layer 1.27mm, inactive germanium layer 0.7mm, and the top cover diameter 72.4mm were entered in the permanent database of the k_0-IAEA program as well as the certificates of the radionuclide (Blaauw, 1993). At the start of the experiment, the background was counted for 3600 seconds.

The single-radionuclide source ^{137}Cs was measured for 1800 sec. at geometry of 17 cm for peak-to-total curve estimation. The mixed peaks (energies) source ^{152}Eu was measured at the three listed distances of 17cm, 15cm and 2cm from the detector end cap for 3600 seconds. The measurements were performed such that the peak statistics in each main peak areas of the radionuclide were better than 0.5%. The minimum chi-square χ_r^2-value of the match for ^{52}Eu between the measured and the computed for all three geometries was 0.9.

3. Results and Discussion

Each curve (Fig. 1-4) of the four techniques employed in measurement of the full energy peak efficiency consists of three parts viz. low energy region below 100 keV which is almost linear, curve above the 100 keV energy region, and linear component as the energy approaches 1000 keV and beyond. All the full energy peak efficiency curves have their highest value around 100 keV and the shapes do not depend on the distance of the photon source from the detector end-cap.   It was also observed from fig. 1-4, that all the full energy peak efficiency data sets had a common turning point around 122keV close to be the maximum value. They was a clear departure of the k_0-IAEA curve from the trend at lower energy of 59.54 keV exhibited by all the other techniques. This was confirmed since the k_0-IAEA software commenced efficiency measurements at 121.78 keV as the lowest energy of ^{152}Eu used. However, lower energy of 59.54 keV may be highly attenuated by the Al end-cap material of the detector cryostat. At higher energy (beyond 200keV), all the techniques agreed very well with the instant effective solid angle derived efficiency data as they all superimposed each other at 2cm and 17cm distances from the detector end-cap (Fig. 1 & 3). This high energy region shows a near linear response in the log-log plot of the full energy peak efficiency data versus energy (Fig 1 & 3). Figure 2 shows high level of superimposition of the three fundamental techniques used for distance 15cm in front of the detector end cap. This is evident as the three techniques ratio perfectly around the unity mark in figure 5 and 6 respectively.

247

Thus, experimental derived efficiency data (values) were employed in the instant effective solid angle derived efficiency technique and full energy peak efficiency data for 1, 5, 10, 15, 20 and 25cm distances were generated as shown in figure 4.   The theoretical (fitted) values over the experimental data were obtained using the semi-empirical least square fit-function described by Eq. (7). The semi-empirical functions with their corresponding fit constants were evaluated for the energy range of 50-200keV, and between 200keV-1408 keV for the three geometries (17cm, 15cm, and 2cm) to take into account the inadequacies of using only single polynomial for the whole energy range of the curve as shown in Table 3.

Insert table (3) about here

The results (Table 4 & 6) of the ratios of the theoretical (fitted) efficiency derived values, experimental efficiency derived data, k_0-IAEA efficiency derived data over the instant effective solid angle efficiency transfer derived data showed a very stable slight oscillations around the unity mark of 0.893 – 1.109 for all three geometries. These fluctuations are observed to exhibit oscillations at some energy with successive maxima and minima as observed in Fig. 5-12. This oscillation posed no problem as it was first noted as being the characteristic of large and medium size Ge-detectors[3]. However, using these ratios, we observed that the instant solid angle efficiency transfer technique agreed very well with the other techniques and was established based on the efficiency data generated accurately at 15cm distance from the detector end-cap.

4.   Conclusions

This work established the concept of evaluating instant efficiency values (curves) once an accurate experimental measurement for a particular geometry is carried out for a given HPGe-detector. This methodology seriously avoids the constant usage of the spectrometry system all the time and the reliability on the radioactive isotopes or radioactive point source employed in efficiency calibration and measurement. Thus, once an experimental accurate data is generated for a particular distance, subsequent derived efficiency data will be developed at any other geometries or distances from the detector end cap. Finally, the work basically revealed the efficiency curve depending not only on the detection crystal but also on the solid angle area generated by the detector active area. However, the four techniques employed in this work have been demonstrated or shown to be very accurate for usage at any point in time since efficiency data/curves are very important in neutron activation analysis.

5.   Acknowledgements

References

ANSI/IEEE, (1996). *IEEE Standard Test Procedures for Germanium Gamma-Ray Detectors, ANSI/IEEE Std. 325* (Inst. of Elect. And Electronics Engineers. Inc., New York. USA).

Blaauw Menno, (1993). *The use of sources emitting coincident γ-rays for determination of absolute efficiency curves of highly efficient Ge detectors.* Nuclear Instruments and Methods in Physics Research A 332 (1993) 493-500.

De Corte F., Dejaeger M., Hossain S. M., Vandenberghe D., De Wispelaere A., Van den Haute P. (2004). *A performance comparison of k0-based ENAA and NAA in the (K, Th, U) radiation dose rate assessment for the luminescence dating of sediments.* Journal of Radioanalytical and Nuclear Chemistry, Vol. 263, No. 3 (2005) 659.665

Debertin, K. and Helmer, R.G. (1988). Gamma-and X-Ray Spectrometry with Semiconductor Detectors. Elsevier Science Publishers B.V.,North-Holland.

Debertin, K., Schötzig, U., Walz, K.F. and Wein, H.M. (1976). *Efficiency Calibration of Semiconductor Spectrometers – Techniques and Accuracies.* Journal of Proceedings, ERDA X-Ray Symp. Ann Arbor, MI P 59-62.

Erdtmann, G., Soyka,W. (1979). *The γ-Rays of the Radionuclides*; Tables for Applied γ-Ray Spectrometry (vol.7). Verlag Chemie: Weinheim, New York, 1-236.

Ewa,I.O.B., Bodizs, D., Czifrus, S., Balla, M., Molnar, Z (2002). *Germanium DetectorEfficiency for a marinelli Beaker Source-Goemetry using the Monte Carlo Method.* Journal of Trace and Microprobe Techniques Vol. 20 (2) P 161-170.

Jonah, S.A., Balogun, G.I.,Umar, M. I., Mayaki, M.C., (2005). *Neutron spectrum parameters in irradiation channels of the Nigeria Research Reactor-1 (NIRR-1) for k_0-NAA standardization.* Journal of Radioanalytical and nuclear chemistry, Vol.266 (1) P 83-88.

Kamboj, S., Kahn, B. (1994). *Intrinsic efficiency calibration of a large germanium detector.* Radioact. Radiochem.5 (2) 46, 56.

Njinga, R.L., Alfa, B., and Ewa, I.O.B. (2009). *Geometry Scaling using HPGe Detector (Model 811-10195) Applied in Neutron Activation Analysis (NAA) Measurements with Nigeria Research Reactor-1 (NIRR-1).* African Journal of Natural Science, Vol. 12, 67-73.

Owens, A. (1989). *A comparison of empirical and semi empirical efficiency calculations for Ge detectors.* Nucl. Instr. Meth. A 274. 297, 304.

Table 1: Radio-nuclides and gamma emission probability used

Radionuclide	Gamma-ray Energy (E), keV	Gamma Emission Probability %
^{241}Am	59.5	35.7
^{226}Ra	351.9	35.10
	609.3	44.26
	1120.3	14.69
^{60}Co	1173.2	99.88
	1332.5	99.98
^{137}Cs	661.6	84.62
^{152}Eu	121.78	28.21
	344.29	26.41
	778.92	13.00
	964.11	14.48
	1112.07	13.55
	1408	20.71

(Erdtmann and Soyka, 1979)

Table 2: Performance Specifications Provided in the Quality Assurance Data Sheet

	Warranted	Measured	Amplifier Time constant
Resolution (FWHM) at 1.33 MeV, ^{60}Co	1.95KeV	1.80KeV	6μs
Peak-to-Compton Ratio, ^{60}Co	54	70.7	6μs
Relative Efficiency at 1.33 MeV, ^{60}Co	30%	43.4%	6μs
Peak Shape (FWTM/FWHM), ^{60}Co	1.98	1.88	6μs
Peak Shape (FWFM/FWHM), ^{60}Co	2.98	2.51	6μs

Table 3: Fit constants data evaluated for the various energy ranges

Constants	Energy $\mu_1$17cm	Energy $\mu_2$17cm	Energy $\mu_1$15cm	Energy $\mu_2$15cm	Energy μ_1 2cm	Energy $\mu_2$2cm
a_0	-181.19	-29.75	-192.19	-26.75	-191.79	-27.75
a_1	100.36	11.43	99.84	12.94	100.36	11.43
a_2	-17.20	-2.44	-18.20	-1.94	-19.70	-2.44
a_3	1.10	0.13	1.17	0.13	1.10	0.13
Regression	0.88	0.90	0.98	0.10	0.98	0.99

where μ_1 represent the region $50 \leq E \leq 200$keV and μ_2 represent the region $200 < E < 1408$ keV

Table 4: Full energy peak efficiency data obtained at 2cm

Gamma-ray Energy (E), keV	$\alpha=k_0$-IAEA efficiency values at d=2cm	β=Experimental efficiency values at d = 2 cm	Ω=Theoretical efficiency values at d = 2 cm	σ=Instant efficiency values at d=2cm	Ratio of α/σ at 2cm	Ratio of β/σ at 2cm	Ratio of Ω/σ at 2cm
59.5	-	8.770E-03	8.100E-03	8.460E-03	-	1.037	0.957
121.78	3.930E-02	3.910E-02	3.930E-02	3.670E-02	1.071	1.065	1.071
344.29	2.100E-02	2.100E-02	2.020E-02	2.120E-02	0.991	0.991	0.953
351.9	-	1.913E-02	1.919E-02	1.961E-02	-	0.976	0.979
609.3	-	1.270E-02	1.276E-02	1.270E-02	-	1.000	1.005
661.6	-	1.170E-02	1.164E-02	1.190E-02	-	0.983	0.978
778.92	1.020E-02	1.019E-02	9.880E-03	1.032E-02	0.988	0.987	0.957
964.11	8.910E-03	9.010E-03	8.470E-03	8.800E-03	1.013	1.024	0.963
1112.07	8.050E-03	7.950E-03	8.490E-03	7.490E-03	1.075	1.061	1.134
1120	-	7.450E-03	8.091E-03	7.641E-03	-	0.975	1.059
1173.2	-	7.390E-03	7.000E-03	7.107E-03	-	1.040	0.985
1332.5	-	6.710E-03	5.990E-03	6.706E-03	-	1.001	0.893
1408	6.220E-03	5.920E-03	5.971E-03	5.990E-03	1.038	0.988	0.997

Table 5: The values of Full energy peak efficiency data obtained at 15cm

Gamma-ray Energy (E), keV	$\alpha=k_0$-IAEA efficiency values at d = 15 cm	β=Experimental efficiency values at d = 15 cm	Ω=Theoretical efficiency values at d = 15 cm	Ratio of α/β at 15 cm	Ratio of Ω/β at 15 cm
59.5	-	6.160E-04	6.590E-04	-	1.070
121.78	3.75E-03	3.680E-03	3.750E-03	1.019	1.019
344.29	2.50E-03	2.580E-03	2.490E-03	0.969	0.965
351.9	-	2.440E-03	2.390E-03	-	0.980
609.3	-	1.780E-03	1.757E-03	-	0.987
661.6	-	1.720E-03	1.660E-03	-	0.965
778.92	1.44E-03	1.510E-03	1.430E-03	0.954	0.947
964.11	1.29E-03	1.270E-03	1.260E-03	1.016	0.992
1112.07	1.13E-03	1.110E-03	1.160E-03	1.018	1.045
1120	-	1.230E-03	1.220E-03	-	0.992
1173.2	-	1.120E-03	1.110E-03	-	0.991
1332.5	-	1.060E-03	9.900E-04	-	0.934
1408	9.64E-04	9.870E-04	1.010E-03	0.977	1.023

Table 6: The values of Full energy peak efficiency data obtained at 17cm

Gamma-ray Energy (E), keV	α= k_0-IAEA efficiency values at d = 17cm	β=Experimental efficiency values at d = 17cm	Ω=Theoretical efficiency values at d = 17cm	σ=Instant efficiency values at d = 17cm	Ratio of α /σ at 17cm	Ratio of β /σ at 17cm	Ratio of Ω /σ at 17cm
59.5	-	4.653E-04	4.650E-04	4.542E-04	-	1.024	1.024
121.78	3.024E-03	2.899E-03	3.010E-03	2.757E-03	1.097	1.052	1.092
344.29	2.118E-03	2.009E-03	2.130E-03	1.933E-03	1.096	1.039	1.102
351.9	-	1.926E-03	1.950E-03	1.890E-03	-	1.019	1.032
609.3	-	1.393E-03	1.390E-03	1.335E-03	-	1.043	1.041
661.6	-	1.270E-03	1.270E-03	1.288E-03	-	0.986	0.986
778.92	1.243E-03	1.193E-03	1.240E-03	1.132E-03	1.098	1.054	1.095
964.11	1.049E-03	1.030E-03	9.850E-04	9.516E-04	1.102	1.082	1.035
1112.07	9.226E-04	8.838E-04	9.120E-04	8.318E-04	1.109	1.063	1.096
1120.3	-	9.531E-04	9.530E-04	9.195E-04	-	1.037	1.036
1173.2	-	9.012E-04	9.010E-04	8.407E-04	-	1.072	1.072
1332.5	-	8.218E-04	8.230E-04	7.988E-04	-	1.029	1.030
1408	7.756E-04	7.118E-04	7.840E-04	7.402E-04	1.048	0.962	1.059

Table 7: The values of Instant Full Energy Peak Efficiency values obtained between 1cm - 25cm

Gamma-ray Energy (E), keV	Instant Full Energy Peak Efficiency values obtained					
	d = 1cm	d = 5 cm	d = 10 cm	d=15cm	d=20cm	d=25cm
59.5	2.187E-02	4.466E-03	1.335E-03	6.160E-04	3.593E-04	2.053E-06
121.78	1.306E-01	2.668E-02	7.973E-03	3.680E-03	2.147E-03	1.227E-05
344.29	9.159E-02	1.871E-02	5.590E-03	2.580E-03	1.505E-03	8.600E-06
351.9	8.662E-02	1.769E-02	5.287E-03	2.440E-03	1.423E-03	8.133E-06
609.3	6.319E-02	1.291E-02	3.857E-03	1.780E-03	1.038E-03	5.933E-06
661.6	6.106E-02	1.247E-02	3.727E-03	1.720E-03	1.003E-03	5.733E-06
778.92	5.361E-02	1.095E-02	3.272E-03	1.510E-03	8.808E-04	5.033E-06
964.11	4.509E-02	9.208E-03	2.752E-03	1.270E-03	7.408E-04	4.233E-06
1112.07	3.941E-02	8.048E-03	2.405E-03	1.110E-03	6.475E-04	3.700E-06
1120	4.367E-02	8.918E-03	2.665E-03	1.230E-03	7.175E-04	4.100E-06
1173.2	3.976E-02	8.120E-03	2.427E-03	1.120E-03	6.533E-04	3.733E-06
1332.5	3.763E-02	7.685E-03	2.297E-03	1.060E-03	6.183E-04	3.533E-06
1408	3.504E-02	7.156E-03	2.139E-03	9.870E-04	5.758E-04	3.290E-06

Table 8: Relationship between Detector active area, Solid Angle and Distances

Geometry d(cm)	Solid Angle Ω(d)	Detector Active Area cm^2	Detector Radius (cm)
1	4.260437688	4.260437688	2.94
2	2.749477113	10.99790845	2.94
3	1.795886519	16.16297867	2.94
4	1.220578373	19.52925397	2.94
5	0.867048462	21.67621154	2.94
6	0.641028945	23.07704202	2.94
7	0.490264448	24.02295797	2.94
8	0.385691495	24.68425566	2.94
9	0.31063516	25.161448	2.94
10	0.255155222	25.5155222	2.94
11	0.213096628	25.78469203	2.94
12	0.180511616	25.99367265	2.94
13	0.154786551	26.1589272	2.94
14	0.134141427	26.29171976	2.94
15	0.11733309	26.39994534	2.94
16	0.103473667	26.48925864	2.94
17	0.091916226	26.56378921	2.94
18	0.082180883	26.62660604	2.94
19	0.07390589	26.68002618	2.94
20	0.06681456	26.72582411	2.94
21	0.060692464	26.76537658	2.94
22	0.055371414	26.79976442	2.94
23	0.050718044	26.8298454	2.94
24	0.046625533	26.85630703	2.94
25	0.043007529	26.87970541	2.94
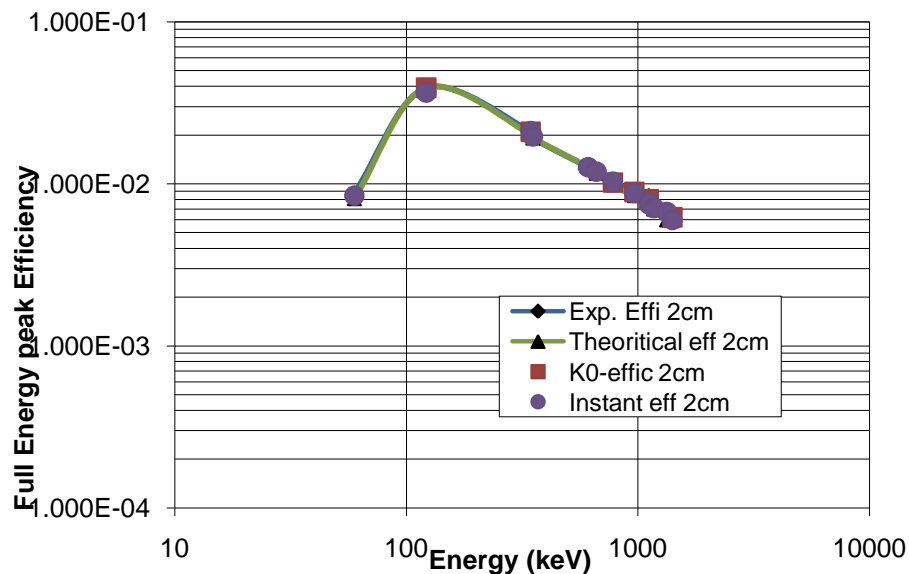
Fig. 1:   Full Energy Efficiency curves obtained at 2cm superimposed each other for all techniques used
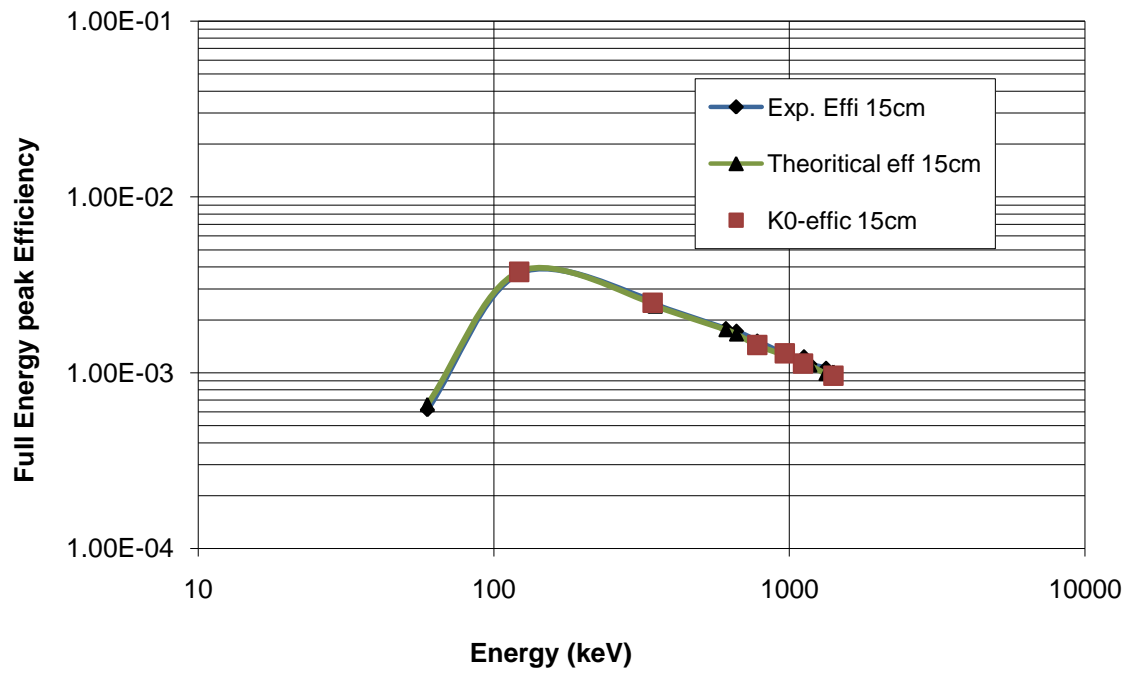
Fig. 2:   The Full Energy Efficiency curves obtained at 15cm superimposed each other for experimental, k0-IAEA, and Theoretical techniques used
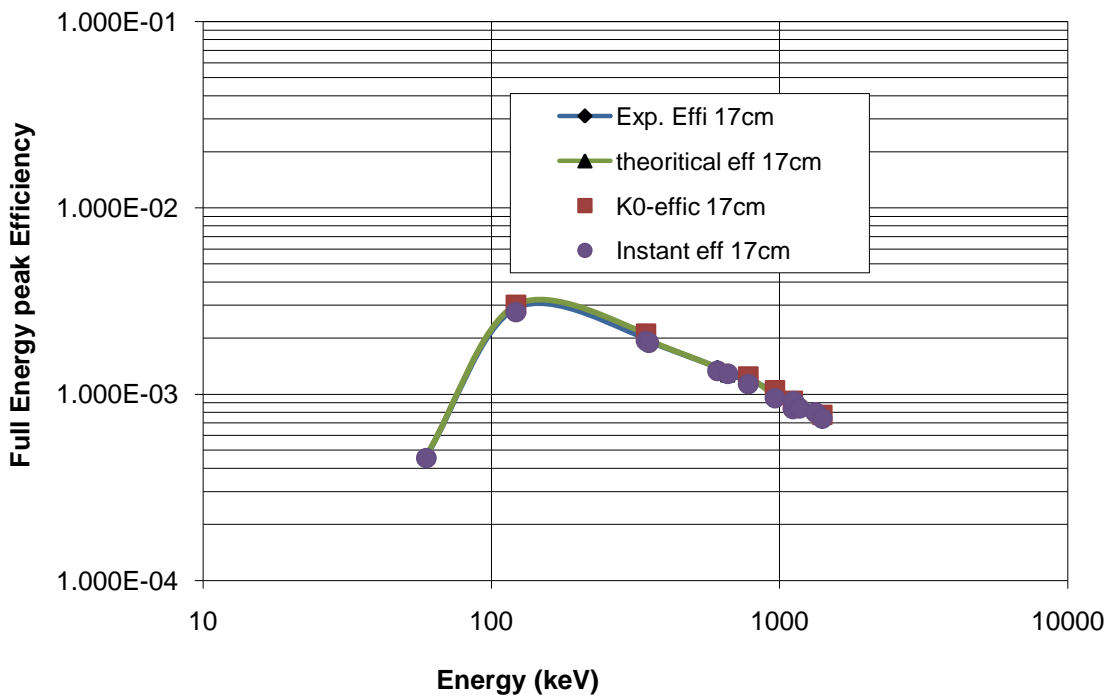
Fig. 3:   The Full Energy Efficiency curves obtained at 17cm superimposed each other for the four different techniques used
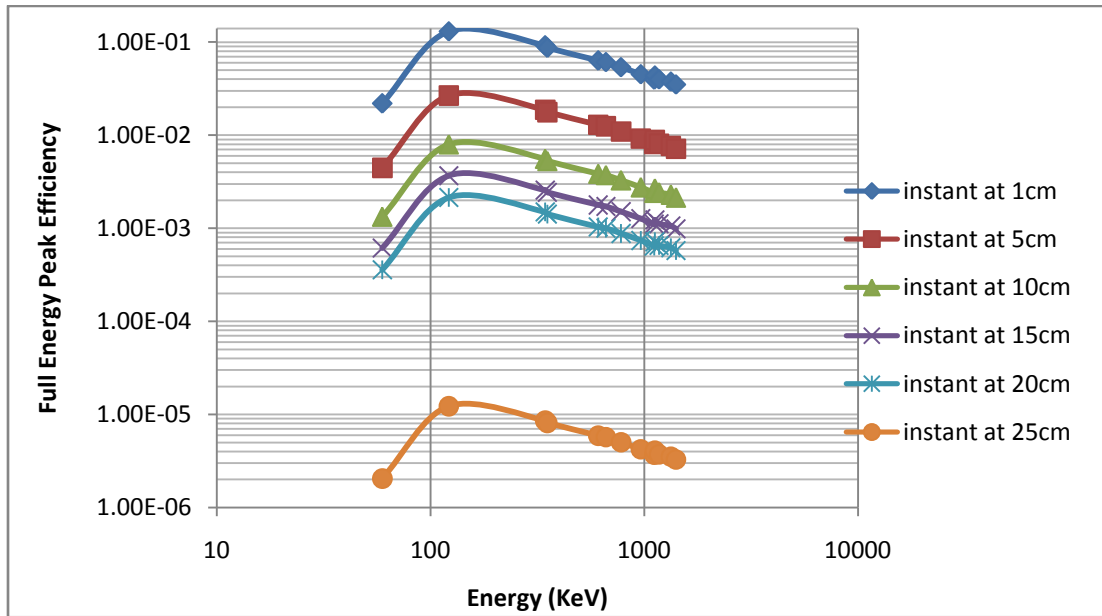
Fig. 4:   The Full Energy Efficiency curves obtained at 1, 5, 10, 15, 20, and 25cm using the instant effective solid angle efficiency transfer technique
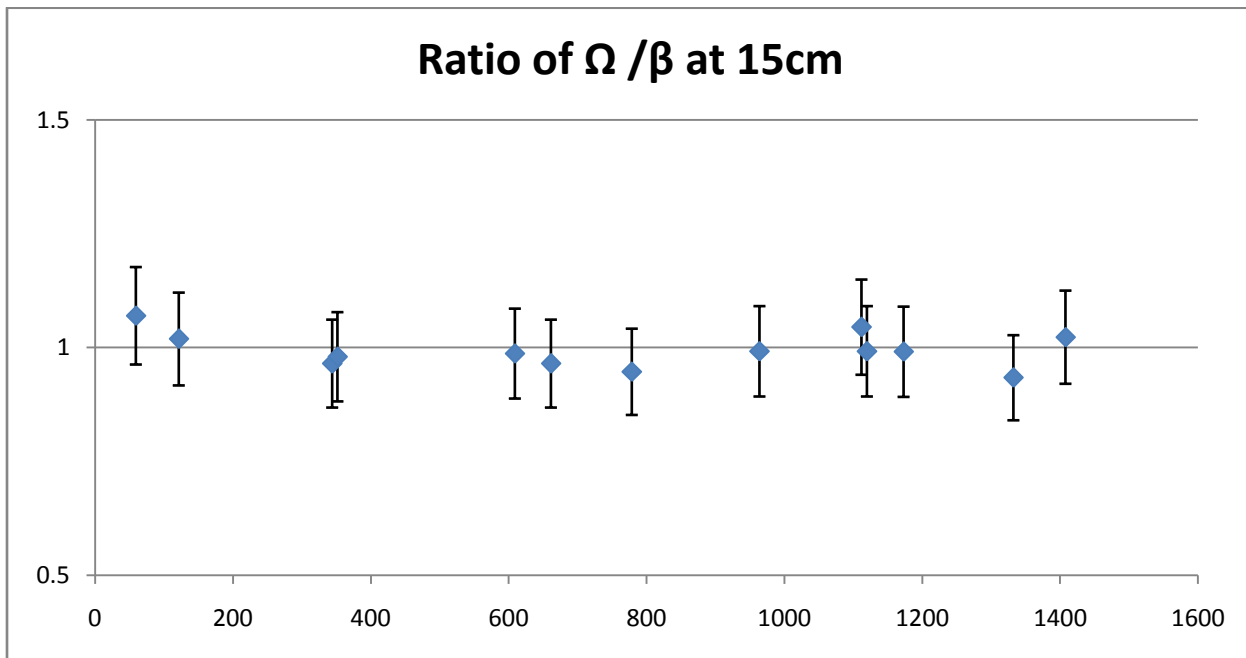

Fig. 5: The ratio of k_0-IAEA efficiency values over Experimental derived efficiency values with error bars of 10% at 15cm
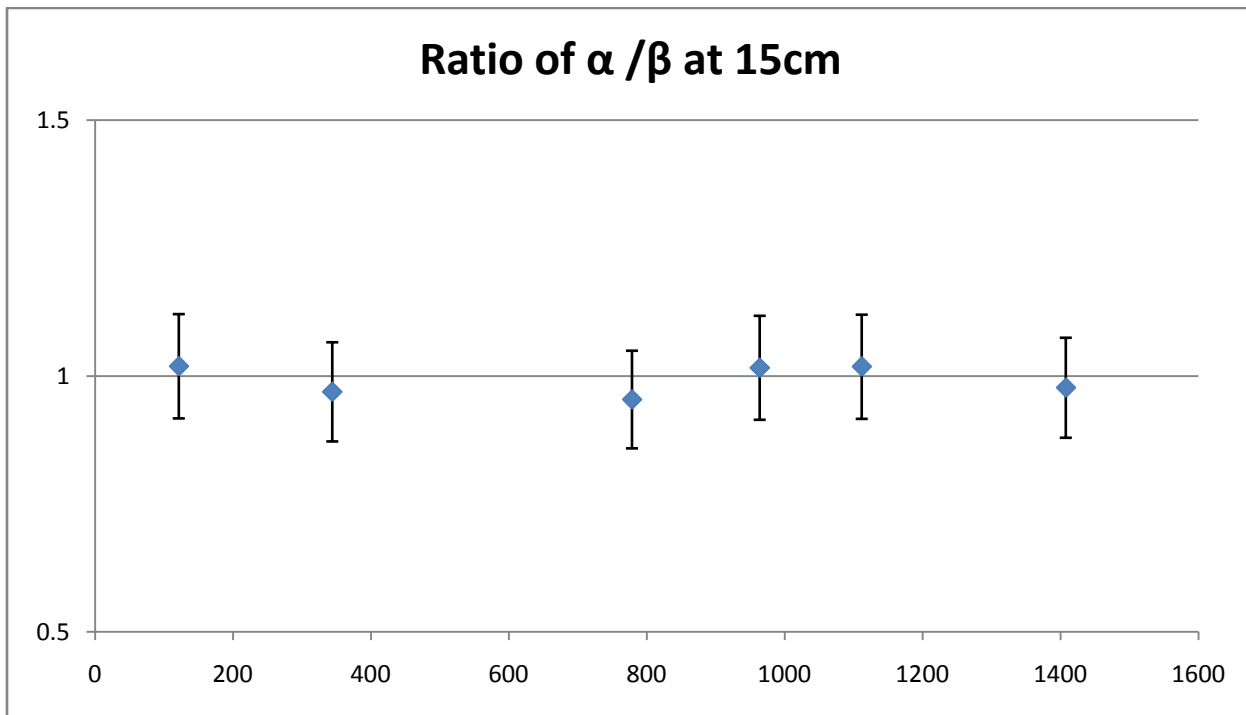
Fig. 6: The ratio of Theoretical derived efficiency values over Experimental derived efficiency values with error bars of 10% at 15cm
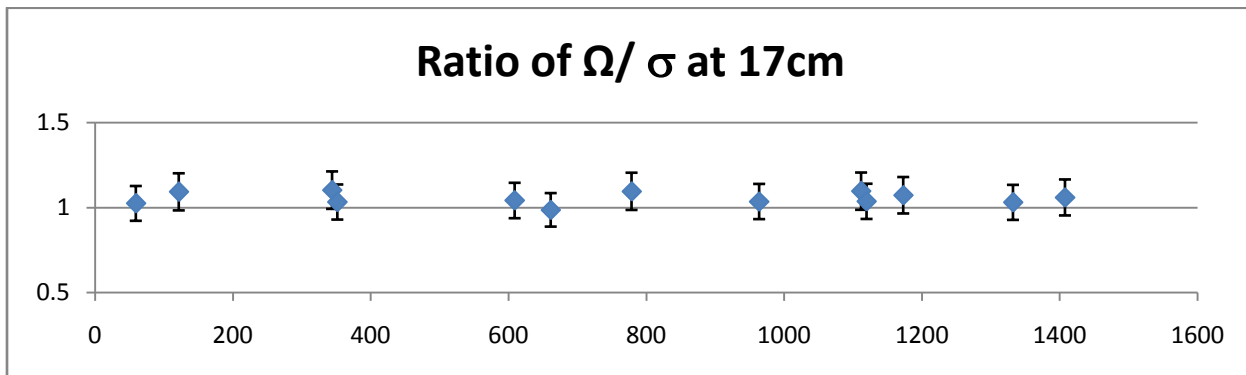
Fig. 7: The ratio of Theoretical derived efficiency values over instant solid angle efficiency transfer derived values with error bars of 10% at 17cm
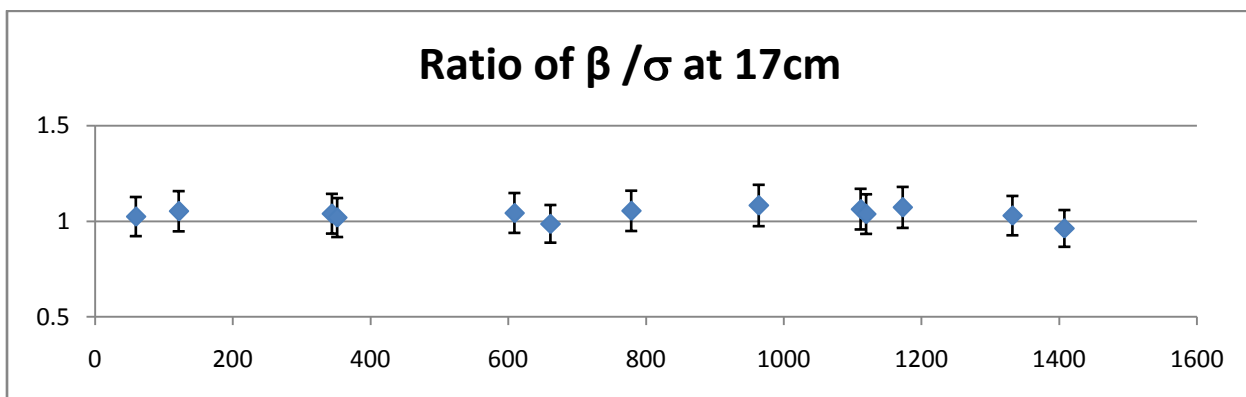
Fig. 8: The ratio of Experimentally derived efficiency values over instant solid angle efficiency transfer derived values with error bars of 10% at 17cm
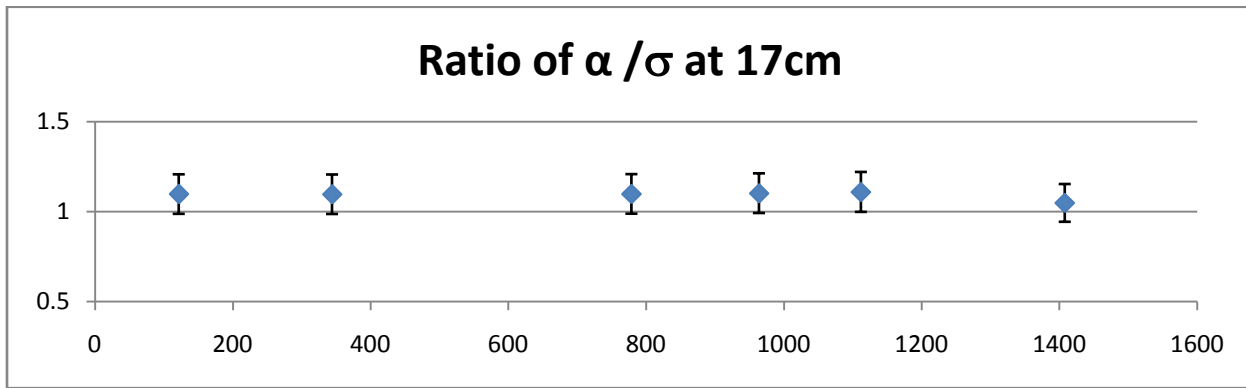
Fig. 9: The ratio of k_o-IAEA software derived efficiency values over instant solid angle efficiency transfer derived values with error bars of 10% at 17cm
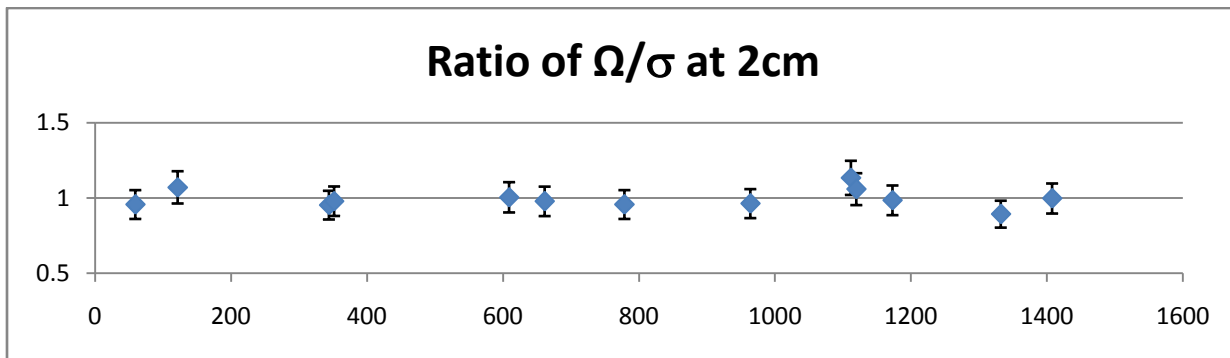

Fig. 10: The ratio of Theoretical derived efficiency values over instant solid angle efficiency transfer derived values with error bars of 10% at 2cm
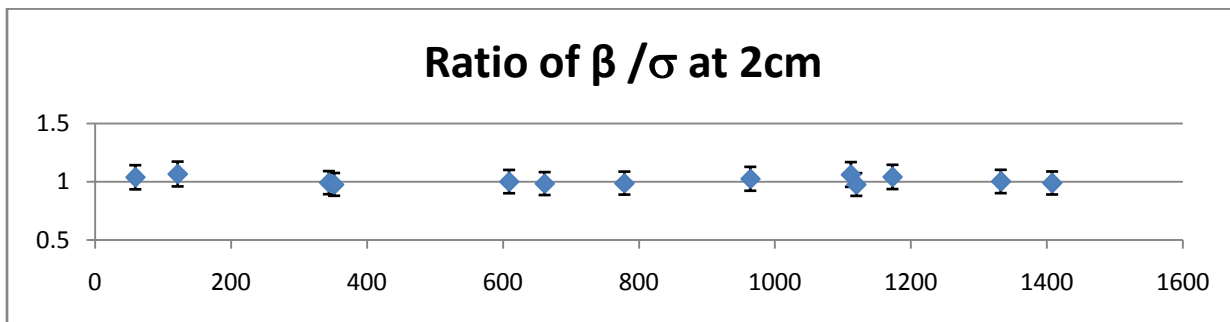

Fig. 11: The ratio of Experimentally derived efficiency values over instant solid angle efficiency transfer derived values with error bars of 10% at 2cm


Fig. 12: The ratio of k_o-IAEA software derived efficiency values over instant solid angle efficiency transfer derived values with error bars of 10% at 2cm